

LETTER TO THE EDITOR

New constraints on the mid-IR EBL from the HESS discovery of VHE γ -rays from 1ES 0229+200

F. Aharonian^{1,13}, A. G. Akhperjanian², U. Barres de Almeida^{8,*}, A. R. Bazer-Bachi³, B. Behera¹⁴, M. Beilicke⁴, W. Benbow¹, K. Bernlöhr^{1,5}, C. Boisson⁶, O. Bolz¹, V. Borrel³, I. Braun¹, E. Brion⁷, A. M. Brown⁸, R. Bühler¹, T. Bulik²⁴, I. Büsching⁹, T. Boutelier¹⁷, S. Carrigan¹, P. M. Chadwick⁸, L.-M. Chounet¹⁰, A. C. Clapson¹, G. Coignet¹¹, R. Cornils⁴, L. Costamante^{1,28}, M. Dalton⁵, B. Degrange¹⁰, H. J. Dickinson⁸, A. Djannati-Atai¹², W. Domainko¹, L. O'C. Drury¹³, F. Dubois¹¹, G. Dubus¹⁷, J. Dyks²⁴, K. Egberts¹, D. Emmanoulopoulos¹⁴, P. Espigat¹², C. Farnier¹⁵, F. Feinstein¹⁵, A. Fiasson¹⁵, A. Förster¹, G. Fontaine¹⁰, Seb. Funk⁵, M. Füßling⁵, Y. A. Gallant¹⁵, B. Giebels¹⁰, J. F. Glicenstein⁷, B. Glück¹⁶, P. Goret⁷, C. Hadjichristidis⁸, D. Hauser¹, M. Hauser¹⁴, G. Heinzlmann⁴, G. Henri¹⁷, G. Hermann¹, J. A. Hinton²⁵, A. Hoffmann¹⁸, W. Hofmann¹, M. Holleran⁹, S. Hoppe¹, D. Horns¹⁸, A. Jacholkowska¹⁵, O. C. de Jager⁹, I. Jung¹⁶, K. Katarzyński²⁷, E. Kendziorra¹⁸, M. Kerschhaggl⁵, B. Khélifi¹⁰, D. Keogh⁸, Nu. Komin¹⁵, K. Kosack¹, G. Lamanna¹¹, I. J. Latham⁸, A. Lemièrre¹², M. Lemoine-Goumard¹⁰, J.-P. Lenain⁶, T. Lohse⁵, J. M. Martin⁶, O. Martineau-Huynh¹⁹, A. Marcowith¹⁵, C. Masterson¹³, D. Maurin¹⁹, G. Maurin¹², T. J. L. McComb⁸, R. Moderski²⁴, E. Moulin⁷, M. de Naurois¹⁹, D. Nedbal²⁰, S. J. Nolan⁸, S. Ohm¹, J.-P. Olive³, E. de Oña Wilhelmi¹², K. J. Orford⁸, J. L. Osborne⁸, M. Ostrowski²³, M. Panter¹, G. Pedalletti¹⁴, G. Pelletier¹⁷, P.-O. Petrucci¹⁷, S. Pita¹², G. Pühlhofer¹⁴, M. Punch¹², S. Ranchon¹¹, B. C. Raubenheimer⁹, M. Raue⁴, S. M. Rayner⁸, M. Renaud¹, J. Ripken⁴, L. Rob²⁰, L. Rolland⁷, S. Rosier-Lees¹¹, G. Rowell²⁶, B. Rudak²⁴, J. Ruppel²¹, V. Sahakian², A. Santangelo¹⁸, R. Schlickeiser²¹, F. Schöck¹⁶, R. Schröder²¹, U. Schwanke⁵, S. Schwarzbürg¹⁸, S. Schwemmer¹⁴, A. Shalchi²¹, H. Sol⁶, D. Spangler⁸, Ł. Stawarz²³, R. Steenkamp²², C. Stegmann¹⁶, G. Superina¹⁰, P. H. Tam¹⁴, J.-P. Tavernet¹⁹, R. Terrier¹², C. van Eldik¹, G. Vasileiadis¹⁵, C. Venter⁹, J. P. Vialle¹¹, P. Vincent¹⁹, M. Vivier⁷, H. J. Völk¹, F. Volpe¹⁰, S. J. Wagner¹⁴, M. Ward⁸, A. A. Zdziarski²⁴, and A. Zech⁶

(Affiliations can be found after the references)

Received 10 August 2007 / Accepted 23 September 2007

ABSTRACT

Aims. To investigate the very high energy (VHE: >100 GeV) γ -ray emission from the high-frequency peaked BL Lac 1ES 0229+200.

Methods. Observations of 1ES 0229+200 at energies above 580 GeV were performed with the High Energy Stereoscopic System (HESS) in 2005 and 2006.

Results. 1ES 0229+200 is discovered by HESS to be an emitter of VHE photons. A signal is detected at the 6.6σ level in the HESS observations (41.8 h live time). The integral flux above 580 GeV is $(9.4 \pm 1.5_{\text{stat}} \pm 1.9_{\text{syst}}) \times 10^{-13} \text{ cm}^{-2} \text{ s}^{-1}$, corresponding to $\sim 1.8\%$ of the flux observed from the Crab Nebula. The data show no evidence for significant variability on any time scale. The observed spectrum is characterized by a hard power law ($\Gamma = 2.50 \pm 0.19_{\text{stat}} \pm 0.10_{\text{syst}}$) from 500 GeV to ~ 15 TeV.

Conclusions. The high-energy range and hardness of the observed spectrum, coupled with the object's relatively large redshift ($z = 0.1396$), enable the strongest constraints so far on the density of the Extragalactic Background Light (EBL) in the mid-infrared band. Assuming that the emitted spectrum is not harder than $\Gamma_{\text{int}} \approx 1.5$, the HESS data support an EBL spectrum $\propto \lambda^{-1}$ and density close to the lower limit from source counts measured by Spitzer, confirming the previous indications from the HEGRA data of 1ES 1426+428 ($z = 0.129$). Irrespective of the EBL models used, the intrinsic spectrum of 1ES 0229+200 is hard, thus locating the high-energy peak of its spectral energy distribution above a few TeV.

Key words. galaxies: BL lacertae objects: individual: 1ES 0229+200 – gamma rays: observations

1. Introduction

The active galactic nucleus (AGN) 1ES 0229+200 was initially discovered in the *Einstein* IPC Slew Survey (Elvis et al. 1992) and later identified as a BL Lac object (Schachter et al. 1993). It is now classified as a high-frequency peaked BL Lac (HBL) due to its X-ray-to-radio flux ratio (Giommi et al. 1995). The HBL is hosted by an elliptical galaxy with absolute magnitude $M_R = -24.53$ (Falomo & Kotilainen 1999), located at a

redshift of $z = 0.1396$ (Woo et al. 2005). Based on its spectral energy distribution (SED) 1ES 0229+200 is suggested as a potential source of VHE γ -rays (Stecker et al. 1996; Costamante & Ghisellini 2002). However, despite several attempts, it has not been previously detected in the VHE regime. The Whipple (de la Calle Perez et al. 2003; Horan et al. 2004), HEGRA (Aharonian et al. 2004a), and Milagro (Williams 2005) collaborations have each reported upper limits on the flux from 1ES 0229+200 during various epochs. The most constraining upper limit (99.9% confidence level) on the flux is $I(>410 \text{ GeV}) < 2.76 \times 10^{-12} \text{ cm}^{-2} \text{ s}^{-1}$, based on ~ 1 h of HESS

* Supported by CAPES Foundation, Ministry of Education of Brazil.

Table 1. The MJD of the first and last night of HESS observations of 1ES 0229+200, the live time of the observations, the number of on- and off-source events measured, the on/off normalization (α), the excess, and the significance of the excess are given. In addition, the integral flux above 580 GeV (assuming $\Gamma = 2.50$), and the corresponding percentage of the Crab Nebula flux above 580 GeV are shown. The χ^2 , degrees of freedom (NDF), and χ^2 probability, $P(\chi^2)$, for a fit of a constant to the flux binned by dark period within each year, or yearly within the total, are also given.

Epoch	MJD First	MJD Last	Time [h]	On	Off	α	Excess	Sig [σ]	$I(>580 \text{ GeV})$ [$10^{-13} \text{ cm}^{-2} \text{ s}^{-1}$]	Crab %	χ^2 , NDF	$P(\chi^2)$
2005	53 614	53 649	6.8	246	2238	0.09160	41	2.7	$6.8 \pm 3.1_{\text{stat}} \pm 1.4_{\text{syst}}$	1.3	1.6, 1	0.21
2006	53 967	54 088	35.0	1344	12304	0.09136	220	6.1	$10.0 \pm 1.7_{\text{stat}} \pm 2.0_{\text{syst}}$	1.9	1.5, 3	0.68
Total	53 614	54 088	41.8	1590	14542	0.09140	261	6.6	$9.4 \pm 1.5_{\text{stat}} \pm 1.9_{\text{syst}}$	1.8	0.8, 1	0.37

observations in 2004 (Aharonian et al. 2005). The present discovery of VHE γ -rays from 1ES 0229+200 makes it the most distant object detected at multi-TeV energies. As a result its VHE spectrum can provide important information on the EBL (Hauser & Dwek 2001) in the mid-infrared band, where few measurements exist.

2. Observations and analysis technique

1ES 0229+200 was observed with the HESS array of imaging atmospheric-Cherenkov telescopes (Hinton 2004) for a total of 70.2 h (161 runs of ~ 28 min each) in 2005 and 2006. After applying the standard HESS data-quality selection, 98 runs remain yielding an exposure of 41.8 h live time at a mean zenith angle $Z_{\text{mean}} = 46^\circ$. The data are calibrated as detailed in Aharonian et al. (2004b) and the standard HESS analysis tools (Benbow 2005) are used. The event-selection criteria are performed using the *standard cuts* (Benbow 2005) resulting in a post-analysis energy threshold of 580 GeV at Z_{mean} . A circular region of radius $\theta_{\text{cut}} = 0.11^\circ$ centered on 1ES 0229+200 is used for the on-source data. The background (off-source data) is estimated using the *Reflected-Region* method (Berge et al. 2007). As the source direction was positioned $\pm 0.5^\circ$ relative to the center of the field-of-view of the camera during the observations, this method allows the simultaneous estimation of the background using the same data as the on-source measurement. The significance of any excess is calculated following the method of Eq. (17) in Li & Ma (1983). The energy of each event passing selection is corrected for the absolute optical efficiency of the system, using efficiencies determined from simulated and observed muons (Aharonian et al. 2006b). This corrects any potential long-term variations in the observed spectrum and flux due to the changing optical throughput of the HESS system. Results consistent with those presented are also found using independent calibration and analysis chains.

3. Results

The results of the HESS observations of 1ES 0229+200 in 2005 and 2006 are shown in Table 1. A significant excess of 261 events (6.6σ) from the direction of 1ES 0229+200 is detected in the total data set. The on-source and normalized off-source distributions of the square of the angular difference between the reconstructed shower position and the source position (θ^2) are plotted in Fig. 1 for all observations. The background is approximately flat in θ^2 as expected, and there is a clear excess at small values of θ^2 corresponding to the observed signal. A two-dimensional fit of the observed excess finds the shape to be characteristic of a point source, located at $(\alpha_{J2000} = 2^{\text{h}}32^{\text{m}}53.2^{\text{s}} \pm 3.1^{\text{s}}_{\text{stat}} \pm 1.3^{\text{s}}_{\text{syst}}, \delta_{J2000} = 20^\circ 16' 21'' \pm 44''_{\text{stat}} \pm 20''_{\text{syst}})$.

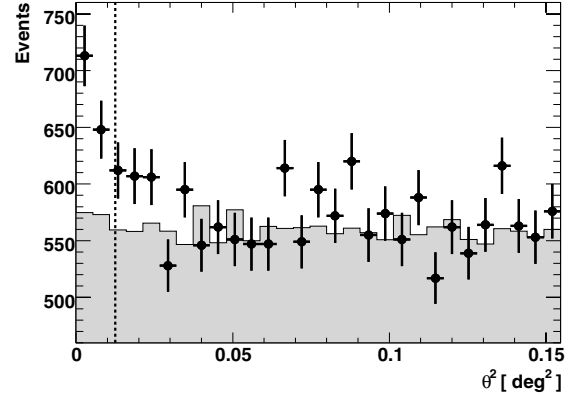


Fig. 1. The distribution of θ^2 for on-source events (points) and normalized off-source events (shaded) from observations of 1ES 0229+200. The dashed line represents the cut on θ^2 applied to the data.

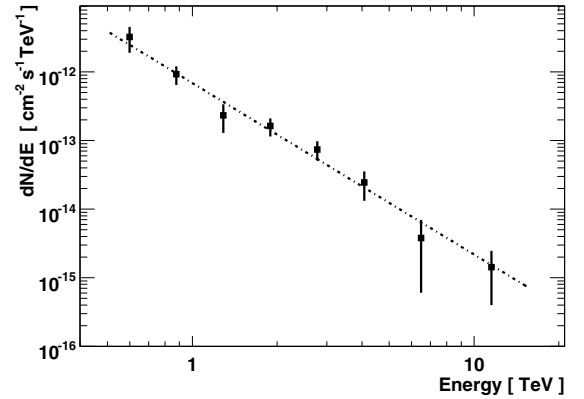


Fig. 2. The VHE spectrum observed from 1ES 0229+200. The line represents the best χ^2 fit of a power law to the observed data. Only the statistical errors are shown.

The excess, named HESS J0232+202, is consistent with the position (Schachter et al. 1993) of the blazar ($\alpha_{J2000} = 2^{\text{h}}32^{\text{m}}48.6^{\text{s}}$, $\delta_{J2000} = 20^\circ 17' 17''$) as expected, and is therefore assumed to be associated with 1ES 0229+200.

Figure 2 shows the time-average photon spectrum observed from 1ES 0229+200. The best χ^2 fit of a power law ($dN/dE \sim E^{-\Gamma}$) to these data yields a photon index $\Gamma = 2.50 \pm 0.19_{\text{stat}} \pm 0.10_{\text{syst}}$, and a χ^2 of 3.6 for 6 degrees of freedom. No evidence for significant features, such as a cutoff or break, are found in the measured spectrum.

Assuming the determined photon index of $\Gamma = 2.50$, the observed integral flux above 580 GeV is $I(>580 \text{ GeV}) = (9.4 \pm 1.5_{\text{stat}} \pm 1.9_{\text{syst}}) \times 10^{-13} \text{ cm}^{-2} \text{ s}^{-1}$. This corresponds to $\sim 1.8\%$ of $I(>580 \text{ GeV})$ measured by HESS from the Crab Nebula

(Aharonian et al. 2006b). Table 1 shows the flux measured during each year of HESS observations. All values are below the previously published VHE upper limits mentioned earlier. The χ^2 and degrees of freedom for fits of a constant to the integral flux versus time when binned by months within each year and years within the total, are also shown in Table 1. As the χ^2 probability for each fit, as well as for fits of the flux binned nightly within each dark period, is greater than 0.2, there is no evidence for variability on any time scale within the HESS data.

4. Discussion

VHE photons from extragalactic sources are expected to suffer absorption from interactions ($\gamma_{\text{VHE}}\gamma_{\text{EBL}} \rightarrow e^+e^-$; Gould & Schröder 1967) with EBL photons (see, e.g., the review of Aharonian 2001). The energy-dependent opacity $\tau(z, E)$ causes a deformation of the observed VHE spectrum ($F_{\text{obs}}(E) = F_{\text{int}}(E) e^{-\tau(z, E)}$) which depends on the EBL SED (Fig. 3). With assumptions about a source's intrinsic VHE spectrum, limits on the EBL density can be derived. Recently, the hard 0.2–2 TeV spectra observed from 1ES 1101–232 and H 2356–309 constrained the EBL around 1–2 μm to a significantly low level, close to the lower limits given by the integrated light from resolved galaxies (Aharonian et al. 2006a, 2007).

Apart from 1ES 1426+428 (Aharonian et al. 2003), 1ES 0229+200 is currently the only VHE source at $z > 0.1$ whose spectrum has been measured up to 10 TeV. Since the peak of the γ - γ cross-section occurs at $\lambda^* \approx 1.4$ ($E_\gamma/1 \text{ TeV}$) μm , these VHE spectra probe the EBL in the near (NIR) to mid-infrared (MIR) range (≈ 2 – $20 \mu\text{m}$), where direct estimates are missing due to increasing foreground emission from interplanetary dust and where EBL models differ significantly in the slope of the SED (Fig. 3). This difference is exemplified by comparison of the models by Primack et al. (2005, hereafter *Prim05*) and Stecker et al. (Stecker, hereafter *Steck06*). Aside from normalization, the NIR-MIR spectrum in the *Prim05* model, as well as in the models by Kneiske et al. (2004), follows the characteristic decline of the old stellar component in the SED of galaxies, which behaves approximately as $\nu I(\nu) \propto \lambda^{-1}$ at these wavelengths. The corresponding photon number density, $n(\epsilon) \propto \epsilon^{-1}$, makes the optical depth almost constant with energy between one and several TeV (Aharonian 2001). This causes a characteristic flattening feature in the attenuation curves. This flattening will be imprinted in the observed VHE spectra for an intrinsic power-law spectrum. In contrast, the EBL decline is much flatter than λ^{-1} for both the *baseline* and *fast evolution* versions of the *Steck06* model. This yields a rapidly increasing opacity above 1 TeV which should translate into a strong and continuous steepening of the observed VHE spectra (unless counterbalanced by upturns in the intrinsic spectrum). It should be noted that, regardless of the EBL model, the optical depth is large (i.e. $\tau > 1$) for all energies relevant here. Therefore, the observed spectrum of 1ES 0229+200 is very sensitive to $\tau(E)$ and hence to the shape of the EBL SED.

The intrinsic spectrum of 1ES 0229+200 can be reconstructed¹ by multiplying the individual data points by $e^{\tau(z, E)}$. For the two *Steck06* models², the 1ES 0229+200

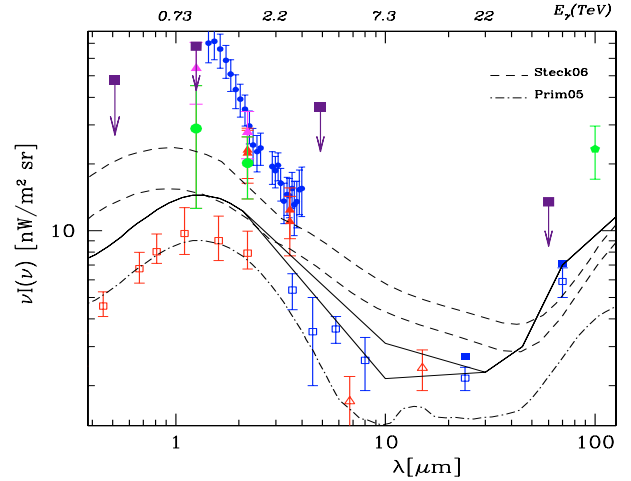


Fig. 3. SED of the EBL at wavelengths most relevant for the VHE spectrum of 1ES 0229+200. The upper axis shows the energy scale corresponding to the peak of the γ - γ cross-section. Data compilation from Aharonian et al. (2006a, see references therein). Open symbols: lower limits given by the integrated light from resolved sources. From left to right: Hubble data (Madau & Pozzetti 2000), Spitzer data (Fazio et al. 2004), ISO data (triangles; Altieri et al. 1999; Elbaz et al. 2002), Spitzer data (Dole et al. 2006). Dashed lines: *fast evolution* (upper) and *baseline* (lower) models of Stecker et al. (2006). Dot-dashed line: model (*Prim05*) of Primack et al. (2005). Solid lines: scaled ($\times 1.6$) *Prim05*, modified above 2 μm by a range of allowed MIR slopes, i.e. those which yield an intrinsic spectrum $\Gamma_{\text{int}} = 1.5$ and $1.15 \approx 1.5 - 0.23_{\text{stat}} - 0.1_{\text{syst}}$. The fluxes at 10 μm are 2.15 and 3.1 $\text{nW m}^{-2} \text{sr}^{-1}$, respectively.

absorption-corrected spectra are well fit by power-law functions ($dN/dE \sim E^{-\Gamma_{\text{int}}}$) with hard photon indices $\Gamma_{\text{int}} = 0.6 \pm 0.3$ (*baseline* EBL) and $\Gamma_{\text{int}} = 0.1 \pm 0.3$ (*fast evolution* EBL). Such hard spectra are not easily explained by commonly used leptonic or hadronic scenarios for the γ -ray emission of BL Lac objects, unless invoking extreme assumptions like mono-energetic particle distributions, either in the shocked plasma (see, e.g., Katarzynski et al. 2006) or as a cold wind with very high ($\sim 10^7$) Lorentz factors (Aharonian et al. 2002). Further, a specific dependence of source parameters on redshift would be required, in order to explain the absence of these hard features in all nearby ($z < 0.1$), less-absorbed VHE-bright HBL.

The *Prim05* model yields $\Gamma_{\text{int}} = 1.92 \pm 0.22$. Since this model falls below the recent lower limits given by Spitzer source counts at MIR (2004; see Fig. 3) wavelengths, and thus underestimates the attenuation at several TeV, modified EBL shapes consistent with the lower limits from source counts are considered in the following.

In standard blazar models, VHE γ -rays are produced by particles accelerated in shocks. For a wide range of conditions the resulting photon spectrum is expected to have $\Gamma_{\text{int}} \gtrsim 1.5$ (Aharonian et al. 2006a). This can be used to constrain the EBL. It should be noted that Stecker et al. (2007) have demonstrated that intrinsic spectra as hard as $\Gamma_{\text{int}} \approx 1.0$ are possible in relativistic shock acceleration scenarios. In such situations, the derived EBL SED constraints will be relaxed. Following Aharonian et al. (2006a), the intrinsic photon spectrum is reconstructed from an EBL SED shape³ and then tested for compatibility

¹ Throughout the paper, a cosmology with $H_0 = 70 \text{ km s}^{-1} \text{ Mpc}^{-1}$, $\Omega_m = 0.3$ and $\Omega_\Lambda = 0.7$ is used for the calculation of $\tau(z, E)$.

² The optical depths were calculated by integrating over the respective EBL SED. The methodology was checked with the prescription in Stecker et al. (2006) for the nearest tabulated redshift ($z = 0.117$), obtaining consistent values ($\Delta\Gamma < 0.05$) for the intrinsic spectrum.

³ In the calculation of τ for these test-SEDs, the effects of galaxy evolution were approximated by modifying the cosmological dependence of the photon number density as $(1+z)^{3-k}$. With $k = 1.2$, the values of $\tau(z)$ are in good agreement with those from the *Prim05* model at $z < 1$. Regardless, evolution effects are small at $z = 0.140$. The difference between including or not this effect is $\Delta\Gamma < 0.08$.

with $\Gamma_{\text{int}} \gtrsim 1.5$. Different EBL shapes can be derived for examination, either by scaling a fixed EBL shape or by changing the NIR/MIR flux ratio (thus testing different EBL slopes).

In the observed energy range of 1ES 0229+200, a simple scaling of EBL SED shapes $\approx \lambda^{-1}$, like the P1.0 curve in Aharonian et al. (2006a) or the *Prim05* shape, does not strongly affect the reconstructed intrinsic spectrum due to the weak energy dependence of the optical depth. Indeed, the spectrum is only modified due to the difference in τ for low and high energy γ -rays, which is not the case here where the EBL mainly causes attenuation. The limit for the overall scaling factor from the HESS 1ES 0229+200 data is $0.8 \times \text{P1.0}$ (i.e. P0.8), or $1.8 \times \text{Prim05}$. The limit on the flux is above those obtained from other VHE sources (Aharonian et al. 2006a).

Different EBL spectral slopes are tested using an EBL template constructed from a fixed scaling of the *Prim05* shape up to $2 \mu\text{m}$ and an interpolation above this wavelength. The MIR-EBL slope is varied using a linear (in log-log scale) interpolation between 2, 10, and $30 \mu\text{m}$, where only the $10 \mu\text{m}$ flux is changed (see Fig. 3). The scaled EBL level is chosen to be $1.6 \times \text{Prim05}$, which corresponds to the EBL upper limit at $1-2 \mu\text{m}$ as derived by Aharonian et al. (2006a). This NIR EBL level allows for the highest possible MIR fluxes, since a high flux at $1-2 \mu\text{m}$ softens the intrinsic spectrum of 1ES 0229+200 in the energy band measured here by HESS. Thus, much higher overall EBL levels are compatible with $\Gamma_{\text{int}} > 1.5$. For a flux at $10 \mu\text{m}$ of $2.15 \text{ nW m}^{-2} \text{ sr}^{-1}$ the intrinsic spectrum is $\Gamma_{\text{int}} = 1.5$. A limiting $10 \mu\text{m}$ flux of $3.1 \text{ nW m}^{-2} \text{ sr}^{-1}$ is derived by taking into account the errors on the photon index (i.e. where $\Gamma_{\text{int}} = 1.15 \approx 1.5 - 0.23_{\text{stat}} - 0.1_{\text{sys}}$). The EBL SED between 2 and $10 \mu\text{m}$ ($\propto \lambda^{-\alpha}$) is thus constrained to a slope $\alpha \gtrsim 1.1 \pm 0.25$. A $\Gamma_{\text{int}} \sim 1.5$ spectrum is also obtained with an EBL SED at the level of the source counts, connecting the optical data points with the Spitzer data at $8 \mu\text{m}$ (for an $\alpha \sim 0.9$). Clearly the HESS data do not support flatter EBL shapes in the MIR, confirming a trend already suggested by the HEGRA data on 1ES 1426+428 (Aharonian et al. 2003).

5. Conclusions

The HESS spectrum of 1ES 0229+200 leads to two important conclusions. First, unless the intrinsic BL Lac spectrum is considerably harder⁴ than 1.5, the EBL density in the MIR range follows a spectrum $\propto \lambda^{-1}$ and is very likely close to the lower limits given by galaxy counts as determined by Spitzer and ISO data. This implies that the sources resolved by Spitzer seem to account for the bulk of the diffuse $5-10 \mu\text{m}$ background. Second, almost independently of the details of the EBL SED, the intrinsic spectrum of 1ES 0229+200 is significantly hard up to $\sim 10 \text{ TeV}$. Thus the high-energy peak of its SED (shown in Fig. 4) is located at energies above a few TeV, among the highest ever seen from a blazar. The extension of the SED to VHE energies provides clear evidence that non-thermal processes are at work in 1ES 0229+200. The SED also includes optical (Bessel *B* and *R* filters) measurements of 1ES 0229+200, $m_R = 16.2$ and $m_B = 17.2$, conducted with the ATOM telescope (Hauser et al. 2004) located at the HESS site. These data are simultaneous with some of the 2006 HESS observations. The ATOM fluxes are constant in time and fall below archival values. Although only limited evidence for a VHE-optical flux correlation exists (Albert et al. 2006), the low optical state might suggest a

⁴ See, e.g., Stecker et al. (2007) for scenarios that demonstrate Γ_{int} as hard as 1.0 is possible in shock acceleration models.

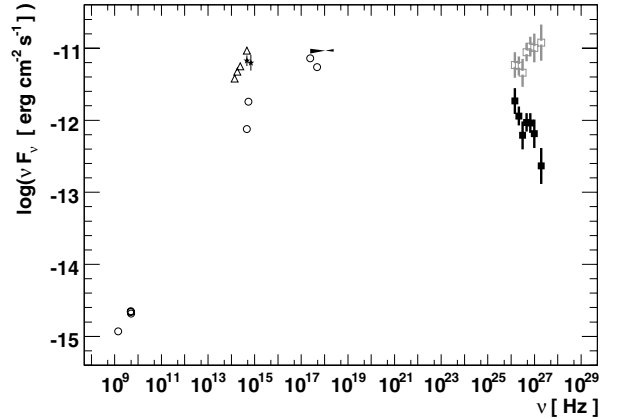


Fig. 4. The broad-band SED of 1ES 0229+200. The ATOM optical measurements (stars) are simultaneous to some of the 2006 HESS data. All other data are non-simultaneous. Both the observed and intrinsic (i.e. de-absorbed with a $1.6 \times \text{Prim05}$ EBL shape, yielding $\Gamma_{\text{int}} = 1.58 \pm 0.22$) VHE spectra are shown, each with the two highest-energy HESS points combined for visibility purposes. Using a lower EBL density results in a softer intrinsic spectrum, but even the very low density of *Prim05* yields $\Gamma_{\text{int}} < 2.0$. The X-ray data are from *Einstein* (2 keV), ROSAT (1 keV; Brinkmann et al. 1995), and BeppoSAX (butterfly; Donato et al. 2005) observations. The radio, NIR (2MASS) and optical data are from the NED archive, Urry et al. (2000), Perlman et al. (1996), and Schachter et al. (1993). The ATOM fluxes and the data marked with open triangles do not have the contribution of the host galaxy subtracted.

correspondingly low VHE state. These results strongly motivate further VHE observations of 1ES 0229+200, as well as contemporaneous observations at lower energies to enable SED modeling.

Acknowledgements. The support of the Namibia authorities and of the University of Namibia in facilitating the construction and operation of HESS is gratefully acknowledged, as is the support by the German Ministry for Education and Research (BMBF), the Max Planck Society, the French Ministry for Research, the CNRS-IN2P3 and the Astroparticle Interdisciplinary Programme of the CNRS, the UK Science and Technology Facilities Council (STFC), the IPNP of the Charles University, the Polish Ministry of Science and Higher Education, the South African Department of Science and Technology and National Research Foundation, and by the University of Namibia. We appreciate the excellent work of the technical support staff in Berlin, Durham, Hamburg, Heidelberg, Palaiseau, Paris, Saclay, and in Namibia in the construction and operation of the equipment. This research has made use of the NASA/IPAC Extragalactic Database (NED) which is operated by the Jet Propulsion Laboratory, California Institute of Technology, under contract with the National Aeronautics and Space Administration.

References

- Aharonian, F. 2001, Proceedings 27th ICRC (Hamburg), Invited, Rapporteur, and Highlight Papers, 250
- Aharonian, F., Timokhin, A., & Plyasheshnikov, A. V. 2002, *A&A*, 384, 834
- Aharonian, F., Akhperjanian, A., Beilicke, M., et al. (HEGRA Collaboration) 2003, *A&A*, 403, 523
- Aharonian, F., Akhperjanian, A., Beilicke, M., et al. (HEGRA Collaboration) 2004a, *A&A*, 421, 529
- Aharonian, F., Akhperjanian, A. G., Aye, K.-M., et al. (HESS Collaboration) 2004b, *Astropart. Phys.*, 22, 109
- Aharonian, F., Akhperjanian, A. G., Bazer-Bachi, A. R., et al. (HESS Collaboration) 2005, *A&A*, 441, 465
- Aharonian, F., Akhperjanian, A. G., Bazer-Bachi, A. R., et al. (HESS Collaboration) 2006a, *Nature*, 440, 1018
- Aharonian, F., Akhperjanian, A. G., Bazer-Bachi, A. R., et al. (HESS Collaboration) 2006b, *A&A*, 457, 899
- Aharonian, F., Akhperjanian, A. G., Bazer-Bachi, A. R., et al. (HESS Collaboration) 2007, *A&A*, 470, 475
- Albert, J., Aliu, E., Anderhub, H., et al. 2006, *ApJ*, 648, L105
- Altieri, B., Metcalfe, L., Kneib, J. P., et al. 1999, *A&A*, 343, L65

- Benbow, W. 2005, Proceedings of Towards a Network of Atmospheric Cherenkov Detectors VII (Palaiseau), 163
- Berge, D., Funk, S., & Hinton, J. 2007, *A&A*, 466, 1219
- Brinkmann, W., Siebert, J., Reich, W., et al. 1995, *A&AS*, 109, 147
- Costamante, L., & Ghisellini G. 2002, *A&A*, 384, 56
- de la Calle Perez, I., Bond, I. H., Boyle, P. J., et al. 2003, *ApJ*, 599, 909
- Dole, H., Lagache, G., Puget, J.-L., et al. 2006, *A&A*, 451, 417
- Donato, D., Sambruna, R. M., & Gliozzi, M. 2005, *A&A*, 433, 1163
- Elbaz, D., Cesarsky, C. J., Chanial, P., et al. 2002, *A&A*, 384, 848
- Elvis, M., Plummer, D., Schachter, J., & Fabbiano, G. 1992, *ApJS*, 80, 257
- Falomo, R., & Kotilainen, J. K. 1999, *A&A*, 352, 85
- Fazio, G. G., Ashby, M. L. N., Barmby, P., et al. 2004, *ApJS*, 154, 39
- Giommi, P., Ansari, S. G., & Micol, A. 1995, *A&AS*, 109, 267
- Gould, R. J., & Schröder, G. P. 1967, *Phys. Rev.*, 155, 1408
- Hauser, M. G., & Dwek, E. 2001, *ARA&A*, 39, 249
- Hauser, M., Möllenhoff, C., Pühlhofer, G., et al. 2004, *Astron. Nachr.*, 325, 659
- Hinton, J. 2004, *New Astron. Rev.*, 48, 331
- Horan, D., Badran, H. M., Bond, I. H., et al. 2004, *ApJ*, 603, 51
- Katarzynski, K., Ghisellini, G., Tavecchio, F., et al. 2006, *MNRAS*, 368, L52
- Kneiske, T. M., Bretz, T., Mannheim, K., & Hartmann, D. H. 2004, *A&A*, 413, 807
- Li, T., & Ma, Y. 1983, *ApJ*, 272, 317
- Madau, P., & Pozzetti, L. 2000, *MNRAS*, 312, L9
- Perlman, E. S., Stocke, J. T., Schachter, J. F., et al. 1996, *ApJS*, 104, 251
- Primack, J. R., Bullock, J. S., & Somerville, R. S. 2005, *AIP Conf. Proc.*, 745, 23
- Schachter, J. F., Stocke, J. T., Perlman, E., et al. 1993, *ApJ*, 412, 541
- Stecker, F. W., de Jager, O. C., & Salamon, M. H. 1996, *ApJ*, 473, L75
- Stecker, F. W., Malkan, M. A., & Scully, S. T. 2006, *ApJ*, 648, 774, with Erratum
- Stecker, F. W., Baring, M. G., & Summerlin, E. J. 2007, *ApJ*, 667, L29
- Urry, C. M., Scarpa, R., O'Dowd, M., Falomo, R., et al. 2000, *ApJ*, 532, 816
- Williams, D. A. 2005, *AIP Conf. Proc.*, 745, 499
- Woo, J. H., Urry, C. M., Van der Marel, R. P., et al. 2005, *ApJ*, 631, 762
- ⁵ Institut für Physik, Humboldt-Universität zu Berlin, Germany
- ⁶ LUTH, Observatoire de Paris, CNRS, Université Paris Diderot, Meudon, France
- ⁷ DAPNIA/DSM/CEA, CE Saclay, Gif-sur-Yvette, France
- ⁸ University of Durham, Department of Physics, UK
- ⁹ Unit for Space Physics, North-West University, Potchefstroom, South Africa
- ¹⁰ Laboratoire Leprince-Ringuet, École Polytechnique, CNRS/IN2P3, Palaiseau, France
- ¹¹ Laboratoire d'Annecy-le-Vieux de Physique des Particules, CNRS/IN2P3, Annecy-le-Vieux, France
- ¹² Astroparticule et Cosmologie (APC), CNRS, Université Paris 7 Denis Diderot, France
- ¹³ Dublin Institute for Advanced Studies, Ireland
- ¹⁴ Landessternwarte, Universität Heidelberg, Königstuhl, Germany
- ¹⁵ Laboratoire de Physique Théorique et Astroparticules, CNRS/IN2P3, Université Montpellier II, France
- ¹⁶ Universität Erlangen-Nürnberg, Physikalisches Institut, Germany
- ¹⁷ Laboratoire d'Astrophysique de Grenoble, INSU/CNRS, Université Joseph Fourier, France
- ¹⁸ Institut für Astronomie und Astrophysik, Universität Tübingen, Germany
- ¹⁹ LPNHE, Université Pierre et Marie Curie Paris 6, Université Denis Diderot Paris 7, CNRS/IN2P3, France
- ²⁰ Institute of Particle and Nuclear Physics, Charles University, Prague, Czech Republic
- ²¹ Institut für Theoretische Physik, Lehrstuhl IV, Ruhr-Universität Bochum, Germany
- ²² University of Namibia, Windhoek, Namibia
- ²³ Obserwatorium Astronomiczne, Uniwersytet Jagielloński, Kraków, Poland
- ²⁴ Nicolaus Copernicus Astronomical Center, Warsaw, Poland
- ²⁵ School of Physics & Astronomy, University of Leeds, UK
- ²⁶ School of Chemistry & Physics, University of Adelaide, Australia
- ²⁷ Toruń Centre for Astronomy, Nicolaus Copernicus University, Toruń, Poland
- ²⁸ European Associated Laboratory for Gamma-Ray Astronomy, jointly supported by CNRS and MPG
-
- ¹ Max-Planck-Institut für Kernphysik, Heidelberg, Germany
e-mail: [Wystan.Benbow;Luigi.Costamante]@mpi-hd.mpg.de
- ² Yerevan Physics Institute, Armenia
- ³ Centre d'Étude Spatiale des Rayonnements, CNRS/UPS, Toulouse, France
- ⁴ Universität Hamburg, Institut für Experimentalphysik, Germany